Mater. Res. Soc. Symp. Proc. Vol. 1203 © 2010 Materials Research Society 1203-J05-03

Characterization of nano-crystalline diamond films grown by continuous DC bias during plasma enhanced chemical vapor deposition

V. Mortet[1,2], L. Zhang[3], M. Eckert[4], A. Soltani[5], J. D'Haen[1,2], O. Douhéret[6], M. Moreau[7], S. Osswald[8], E. Neyts[4], D. Troadec[5], P. Wagner[1,2], A. Bogaerts[4], G. Van Tendeloo[3], K. Haenen[1,2].

[1] Institute for Materials Research (IMO), Hasselt University, Diepenbeek, Belgium.
[2] Division IMOMEC, IMEC vzw, Diepenbeek, Belgium.
[3] Electron Microscopy for Materials Science (EMAT), University of Antwerp, Antwerpen, Belgium.
[4] Research group PLASMANT, Department of Chemistry, University of Antwerp, Antwerp, Belgium.
[5] Institut d'Electronique de Microélectonique et de Nanotechnologie, Villeneuve d'Ascq, France.
[6] Service de la Chimie des Materiaux Nouveaux, MateriaNova Research Center, Mons, Belgium.
[7] Laboratoire de Spectrochimie Infrarouge et Raman, Villeneuve d'Ascq, France.
[8] Department of Materials Science and Engineering and A. J. Drexel Nanotechnology Institute, Drexel University, Philadelphia, USA

ABSTRACT

Nanocrystalline diamond films have generated much interested due to their diamond-like properties and low surface roughness. Several techniques have been used to obtain a high re-nucleation rate, such as hydrogen poor or high methane concentration plasmas. In this work, the properties of nano-diamond films grown on silicon substrates using a continuous DC bias voltage during the complete duration of growth are studied. Subsequently, the layers were characterised by several morphological, structural and optical techniques. Besides a thorough investigation of the surface structure, using SEM and AFM, special attention was paid to the bulk structure of the films. The application of FTIR, XRD, multi wavelength Raman spectroscopy, TEM and EELS yielded a detailed insight in important properties such as the amount of crystallinity, the hydrogen content and grain size. Although these films are smooth, they are under a considerable compressive stress. FTIR spectroscopy points to a high hydrogen content in the films, while Raman and EELS indicate a high concentration of sp^2 carbon. TEM and EELS show that these films consist of diamond nano-grains mixed with an amorphous sp^2 bonded carbon, these results are consistent with the XRD and UV Raman spectroscopy data.

INTRODUCTION

In all times, its excellent properties have always stirred up the interest for diamond. Due to the excellent mechanical properties of this material, smooth nano-diamond thin films could be applied in micro-electro-mechanical systems (MEMS) [1]. Moreover, nano-diamond particles have generated an intense interest in microbiology [2,3] as, for instance, active biocompatible bio-markers. While nano-diamond thin films, i.e. films made of diamond nano particles embedded in an amorphous and non diamond carbon phase, are produced by chemical vapor deposition (CVD) techniques, the most used technique to produce nano-diamond particles is based on a detonation process, which is a cumbersome and hard to control industrial process [2].

On the other hand, the use of substrate bias has been proven to be an efficient method for diamond nucleation and it has been extensively studied. Although nano-diamond thin films grown with substrate bias have been reported in the past [4,5,6]. The recent renewal of interest in nano-diamond and the development of characterization methods urges for new and more elaborate studies.

EXPERIMENTAL

Films were grown on 10 mm in diameter silicon substrates by microwave (MW) plasma enhance (PE) CVD in a NIRIM type reactor [7] during one hour using a 1% mixture of methane diluted in hydrogen. The 15 mm in diameter substrate holder is negatively biased at 260 V. A 40 mm in diameter, grounded stainless steel tube around the substrate holder serves as a counter electrode. Prior to the growth, the sample is first heated to 700°C in a pure hydrogen plasma. Second, the sample is bias enhanced nucleated at a pressure of 50 mbar, a power of 275 W and a negative bias voltage of 260 V using a 1% methane to hydrogen mixture for 10 minutes. The film is then grown under the same bias at a pressure of 80 mbar and a power of 425 W. The samples were characterized by scanning electron microscopy (SEM), atomic force microscopy (AFM), X-ray diffraction (XRD), transmission electron microscopy (TEM), electron energy loss spectroscopy (EELS), and Raman spectroscopy using multiple excitation wavelengths, from infrared (785 nm) to ultraviolet (266 nm).

RESULTS

The mass deposition rate of the films, which show a black and glassy surface (see inset Fig. 1), is high (2 $mg.cm^{-2}.h^{-1}$ – 5.2 $\mu m.h^{-1}$), that is nearly 8 times higher than the obtained deposition rate without the application of bias. The large curvature of the sample suggests a high compressive stress. Assuming that there is no plastic deformation of the substrates, a compressive stress higher than 20 GPa has been calculated using the Stoney's equation. These results are similar to the ones reported by Sharda et al. [8].

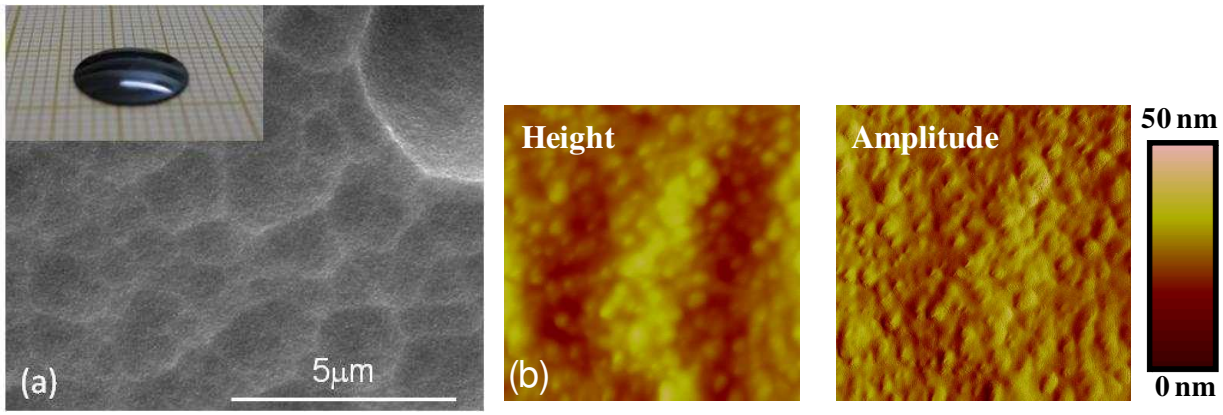

Figure 1. (a) Scanning electron microscopy image of a film grown under a negative DC bias of 260 V– inset: picture of the film. (b) Atomic force microscope images, obtained in tapping mode, of the film on a 500 nm x 500 nm surface.

The surface morphology of the film observed by SEM and AFM is shown in Fig. 1. The surface is smooth (fig. 1a) and a fine structure can be observed by AFM (fig. 1b). The surface roughness is R_{ms} ~ 4-5 nm on a 500 nm x 500 nm surface area, while the observed grain size, which is a convolution of the real grain size and the size of the probing tip, is estimated to be around 20 to 40 nm.

The X-ray diffraction diagram (Fig. 2) of the film only exhibits the diffraction peaks of diamond and the silicon (100) substrate. The diamond peaks are wide and low in intensity. Using the Scherrer's equation with Gaussian and Lorentzian fittings of the peaks, the coherence length of the diamond crystals has been estimated to be 5-6 nm. The diffraction diagram of a 4 nm grain sized powder is also shown on Fig. 2 for comparison.

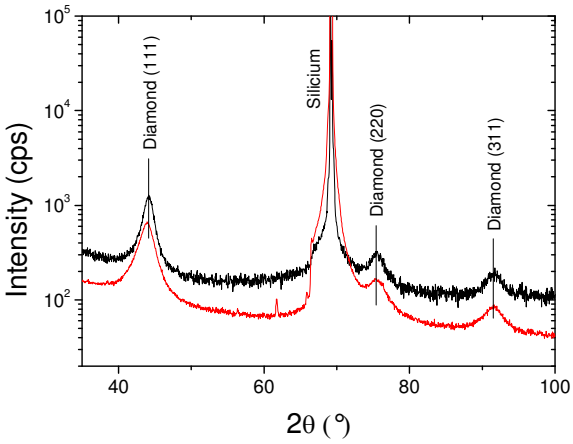

Figure 2. X-ray diffraction diagrams of nano-diamond thin film grown under a negative DC bias of 260 V (upper / black curve) and nano-crystalline diamond powder with a grain size of 4 nm (lower / red curve).

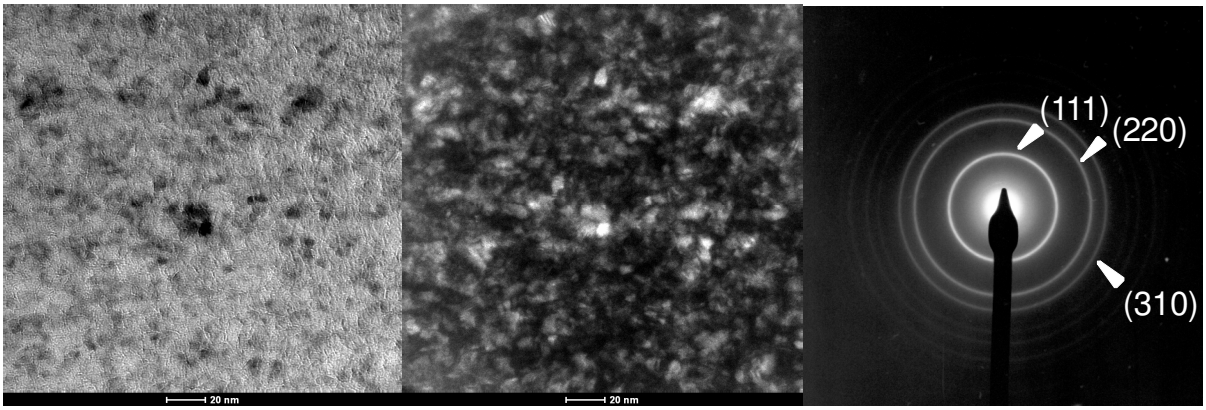

(a) (b) (c)

Figure 3. (a) bright field and (b) conical dark field, using the (111) diffraction ring, transmission electron microscopy images and (c) electron diffraction pattern of a nano-diamond thin film grown under a negative DC bias.

The TEM and the electron diffraction pictures (see Fig. 3) support the results obtained by XRD. The dark field image clearly shows that the films consist of nanometer size (~10 nm in

average) diamond grains. The sp^3 to amorphous carbon ratio was computed from the EELS spectrum (not shown) and it was determined to be ~ 81%. Raman scattering spectra obtained with different wavelength excitations in the first order range are shown in Fig. 4a. Infra-red and visible Raman scattering spectra exhibit only the graphite (G) band, the disordered graphitic (D) band, and a shoulder at ~ 1150 cm^{-1}. Despite polyacetylene is known to decompose around 400°C, the band at 1150 cm^{-1} is generally assigned to trans-polyacetylene [9-11].

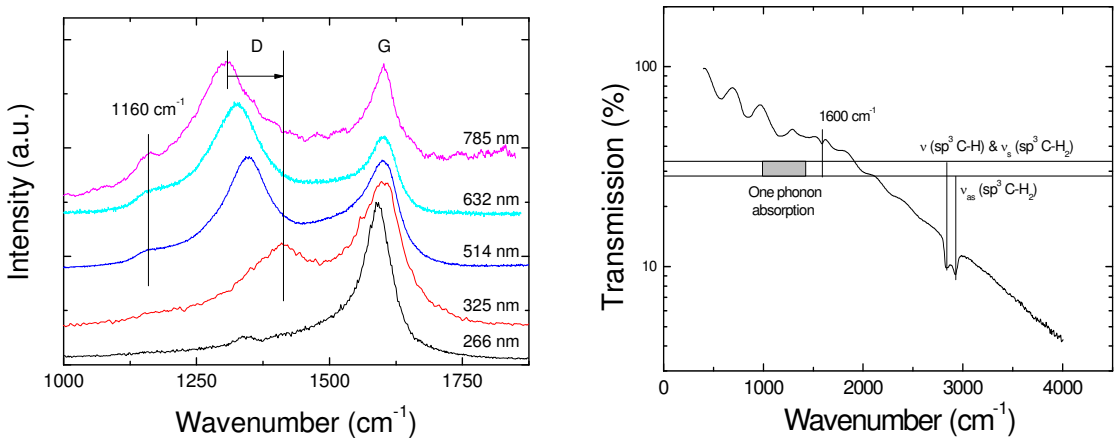

Figure 4. (a) Raman scattering spectra of the nano-diamond films obtained using different excitation wavelengths; 266 nm, 325nm, 514 nm, 632 nm and 785 nm; (b) infra-red transmission of a nano-diamond film in a semi-log plot (b).

The D band, that is due to double Raman resonant scattering [12,13], decreases in relative intensity vs the G band while shifting to higher wavenumbers at a rate of ~ 60 cm^{-1}/eV as the photon energy (E_{ph}) of the excitation laser increases. The D band, that should be located at 1495 cm^{-1}, is not significantly observed in UV Raman scattering at E_{ph} = 4.66 eV (266 nm). Nonetheless, the tail at lower wavenumbers of the G band might be due to the D band. The UV Raman spectrum shows, besides the G band, a minute and relatively broad band at 1341 cm^{-1}. Raman scattering of nanometer sized diamond grains has already been reported [14, 15]. The diamond band shifts to lower wavelength and broadens as the grain size decreases due to phonon confinement [16]. Yoshikawa et al. [14] have reported a red shift of 13 cm^{-1} and a width of 38 cm^{-1} on detonation diamond with a grain size of 5 nm. The diamond band is also known to shift to higher wavelengths when the material is under compressive stress at a rate of 2.9 cm^{-1}/GPa [17]. Thus, the tiny band at 1341 cm^{-1} is not assigned to the D band but to nano-diamond under compressive stress. The diamond grain size has been estimated to be 7-8 nm and a compressive stress of σ ~ 6.5 GPa is calculated, assuming the peak position of non-stressed nano-diamond to be at 1322 cm^{-1}.

Fig. 4b shows the infrared absorption spectrum of a nano-diamond film. In addition to the thickness interference fringes at low wavelengths (ν < 2000 cm^{-1}) and the increasing absorption with wavenumbers due to the presence of graphitic carbon, three significant absorptions bands are observed: between 950 and 1400 cm^{-1} (band I) , at 1600cm^{-1} (band II) and between 2800 and 3000 cm^{-1} (band III). The band III is a convolution of different absorption bands of sp^3 CH_x bonds' stretching vibration modes: the symmetric $\nu_{as}(sp^3\ CH_2)$ ~2850 cm^{-1} and antisymmetric $\nu_{as}(sp^3\ CH_2)$ ~ 2920 cm^{-1} modes of CH_2 [18] and the CH vibration at $\nu_{as}(sp^3\ CH)$ ~ 2830 cm^{-1}

present on the (111) surface of diamond [19]. Using a thin film of polyethylene for the calibration of the CH_2 antisymmetric vibration mode absorption, the atomic concentration of hydrogen in the film is assumed to be higher than 3 x 10^{22} cm^{-3}. This level of hydrogen is in accordance with other reports on hydrogen concentration in nano-crystalline diamond films [5,20]. High concentrations of hydrogen are generally observed in nano-diamond. It is assumed to be trapped at grain boundaries, thus its concentration increases as the grain size decreases [20]. Classical Molecular Dynamics modeling shows a large increase of dangling bonds formation at high bias voltages that is assumed to enhance the reactivity of the material [20]. It is believed that these dangling bonds contribute to the large deposition rate and the high concentration of hydrogen in the films. The band II is ascribed to either conjugated C=C bonds in polyene, or aromatics rings [21]. The presence of C=C bonds in nano-diamond thin films is in accordance with the HR-EELS results of Michaelson and Hoffman [22]. The band I is attributed to both the one phonon absorption of diamond and the absorption of the deformation (δ) vibration mode of sp^3 CH_x groups. The presence of this CH_x deformation's absorption band is consistent with the high concentration of hydrogen in the film determined through the absorption of CH_2 stretching vibration modes. Furthermore, the CH bending vibration mode has been also observed by HR-EELS on nano-diamond films [22]. Although the one phonon absorption is normally forbidden in diamond, the rule breaks in case of diamond grains of very small size [23]. One can also notice that absorption bands of trans-polyacetylene at ~1000 cm^{-1}, 1800 cm^{-1} and ~3045 cm^{-1} are not observed on the IR transmission spectrum, and the Raman band at 1160 cm^{-1} does not significantly shift with the excitation energy as expected for trans-polyacetylene [24]. Nonetheless, this band has to be assigned to a CH vibration mode as it has been shown by deuteration experiments [22]. Thus, it is strongly believed that this band has to be assigned to a deformation mode of CH_x bonds only.

CONCLUSIONS

Structural properties of diamond thin films grown by continuously bias assisted MW PE CVD have been characterized using different techniques. All characterization methods confirm that nano-crystalline diamond films have been grown. The films consist of nano-diamond grains of ~ 10 nm in size mixed with amorphous sp^2 bonded carbon. They are under large compressive stress and present a high concentration of hydrogen. Visible and IR Raman scattering results show only the signature of sp^2 bonded carbon while the diamond signature is only observed using UV excitation scattering. Furthermore, these results disagree with previous reports, which conclude that the Raman scattering band at ~1150 cm^{-1} is due to trans-polyacetylene. In contrast, it is proposed that the origin of this band can be considered to be a deformation mode of CH_x bonds

ACKNOWLEDGMENTS

This work was financially supported by the Research Programs G.0068.07 and G.0430.07 of the Research Foundation - Flanders (FWO), the Methusalem "NANO network Antwerp-Hasselt", and the IAP-P6/42 project 'Quantum Effects in Clusters and Nanowires'.

REFERENCES

1. O.A. Williams, M. Nesládek, M. Daenen, Sh. Michaelson, A. Hoffman, E. Ōsawa, K. Haenen, R.B. Jackman, Diamond Relat. Mater. **17**, 1080 (2008).
2. A. Krueger, Advanced Mater. **20**, 2444 (2008).
3. H. Huang, Pierstorff, E. Osawa, D. Ho, Nano Lett. **7**, 3305 (2007).
4. N. Jiang, K. Sugimoto, K. Eguchi, T. Inaoka, Y. Shintani, H. Makita, A. Hatta, A. Hiraki, J. Cryst. Growth **222**, 591 (2001).
5. M. Schreck, T. Baur, R. Fehling, M. Muller, B. Stritzker, A. Bergmaier, G. Dollinger, Diamond Relat. Mater. **7**, 293 (1998).
6. C.Z. Gu, X. Jiang, J. Appl. Phys. **88**, 1788 (2000).
7. V. Mortet, M. Daenen, T. Teraji, A. Lazea, V. Vorlicek, J. D'Haen, K. Haenen, M. D'Olieslaeger, Diamond Relat. Mater. **17**, 1330 (2008).
8. T. Sharda, T. Soga, T. Jimbo, M. Umeno, Diamond Relat. Mater. **10**, 352 (2001).
9. A.C. Ferrari, J. Robertson, Phys. Rev. B **63** (2001) 121405(R).
10. H. Kuzmany, R. Pfeiffer, N. Salk, B. Gunther, Carbon **42** (2004) 911.
11. T. Lopez-Rios, E. Sandre, S. Leclercq, E. Sauvain, Phys. Rev. Lett. **76** (1996) 4935.
12. S. Reich, C. Thomsen, Phil. Trans. R. Soc. Lond. A **362**, 2271 (2004).
13. C. Thomsen, S. Reich, Phys. Rev. Lett. **85**, 5214 (2000).
14. M. Yoshikawa, Y. Yuri, M. Maegawa, G. Katagiri, H Ishida, A. Ishitani, Appl. Phys. Lett. **62**, 3114 (1993).
15. J. Chen, S.Z. Deng, J. Chen, Z.X. Yu, and N.S. Xu, Appl. Phys. Lett. **74**, 3651 (1999).
16. R.J. Nemanich, S.A. Solin, R. M. Martin, Phys. Rev. B **23**, 6348 (1981).
17. H. Boppart, J. van Straaten, I. Silver, Phys. Rev. B **32**, 1423 (1985).
18. G. Socrates, Infrared and Raman characteristic group frequencies – tables and charts, 3rd ed. (John Weiley & Sons Ltd, Chichester, 2001) p. 50.
19. B.F. Mantel, M. Stammler, J. Ristein, L. Ley, Diamond Relat. Mater. **9**, 1032 (2000).
20. Sh. Michaelson, O. Ternyak, R. Akhvlediani, O.A. Williams, D. Gruen, A. Hoffman, Phys. Stat. Sol. (a) **204**, 2860 (2007).
21. Bernhard Schrader, Infrared and Raman spectroscopy – Methods and applications (VCH Verlagsgesellschaft mbH, Weinheim, 1995), p.197-199.
22. Sh. Michaelson and A. Hoffman, Diamond Relat. Mater. **15**, 486 (2006).
23. P. K. Bachmann and D. U. Wiechert, Diam. Relat. Mater. **1**, 422 (1992).
24. J.-Y. Kim, E.-R. Kim, D.-W. Ihm, M. Tasumi, Bull. Korean Chem. Soc. **23**, 1404 (2002).